

On the magnitude of the electrostatic contribution to ligand–DNA interactions

VINOD K. MISRA AND BARRY HONIG

Department of Biochemistry and Molecular Biophysics, Columbia University, 630 West 168th Street, New York, NY 10032

Communicated by Harold A. Scheraga, Cornell University, Ithaca, NY, December 12, 1994

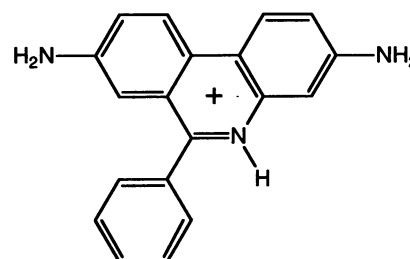
ABSTRACT A model based on the nonlinear Poisson–Boltzmann equation is used to study the electrostatic contribution to the binding free energy of a simple intercalating ligand, 3,8-diamino-6-phenylphenanthridine, to DNA. We find that the nonlinear Poisson–Boltzmann model accurately describes both the absolute magnitude of the pK_a shift of 3,8-diamino-6-phenylphenanthridine observed upon intercalation and its variation with bulk salt concentration. Since the pK_a shift is directly related to the total electrostatic binding free energy of the charged and neutral forms of the ligand, the accuracy of the calculations implies that the electrostatic contributions to binding are accurately predicted as well. Based on our results, we have developed a general physical description of the electrostatic contribution to ligand–DNA binding in which the electrostatic binding free energy is described as a balance between the coulombic attraction of a ligand to DNA and the disruption of solvent upon binding. Long-range coulombic forces associated with highly charged nucleic acids provide a strong driving force for the interaction of cationic ligands with DNA. These favorable electrostatic interactions are, however, largely compensated for by unfavorable changes in the solvation of both the ligand and the DNA upon binding. The formation of a ligand–DNA complex removes both charged and polar groups at the binding interface from pure solvent while it displaces salt from around the nucleic acid. As a result, the total electrostatic binding free energy is quite small. Consequently, nonpolar interactions, such as tight packing and hydrophobic forces, must play a significant role in ligand–DNA stability.

Understanding the factors that drive simple ligand–DNA interactions provides general insights into the requirements for stable and specific nucleic acid recognition. The principal contributions to the free energy of association of ligands with nucleic acids can be divided into polar (electrostatic) and nonpolar terms, where the nonpolar contribution includes hydrophobic interactions, van der Waals interactions, and translation, rotational, and configurational entropies (1). Proton binding is a sensitive probe of electrostatic effects on ligand–DNA interactions (2). The change in the pK_a of a single titrating group on a ligand upon binding (the pK_a shift; ΔpK_a) is a measure of the difference in the electrostatic contribution to the binding free energy of the charged and neutral ligands, $\Delta\Delta G_{el}$ (see Scheme I). As such, ΔpK_a can be used to verify the accuracy of any theoretical model used to calculate the electrostatic contribution to ligand–DNA binding.

The Poisson–Boltzmann (PB) equation provides an accurate description of many electrostatic phenomena in macromolecular systems (1, 3). However, most applications to date have focused on weakly charged macromolecules for which linearized solutions to the PB equation are valid. In contrast, the high charge density of the phosphodiester backbone of nucleic acids necessitates the use of the full nonlinear PB (NLPB)

equation (4), which has been recently shown to reproduce accurately the salt dependence of the binding constant for several minor-groove-binding antibiotics and DNA-binding proteins (5–7). In this paper, we will show that the NLPB equation provides a very accurate method for calculating the absolute magnitude of the total electrostatic binding free energy, $\Delta\Delta G_{el}$, as well.

The intercalation of 3,8-diamino-6-phenylphenanthridine (DAPP; its protonated structure is shown below) into DNA



results in a stabilization of the protonated state of the antibiotic in the bound form (2). This is manifested as an upward shift in the pK_a of DAPP upon binding. In addition, the observed pK_a shift is a linear function of the logarithm of the univalent salt concentration (2). As the salt concentration increases, the magnitude of the pK_a shift decreases. In this paper, we will use these observations to test the accuracy of the NLPB model for calculating the total electrostatic free energy of highly charged systems as a function of univalent salt concentration. We will then analyze our findings to delineate the role of electrostatics in the binding of a simple ligand to DNA.

METHODS

Theory. Calculation of the total electrostatic free energy. The total electrostatic free energy of a molecule, ΔG_{el} in a univalent salt solution can be determined from the NLPB equation:

$$\nabla \cdot [\epsilon(\mathbf{r}) \nabla \cdot \phi(\mathbf{r})] - (8\pi e^2 I / kT) \sinh[\phi(\mathbf{r})] + 4\pi e \rho^f(\mathbf{r}) / kT = 0, \quad [1]$$

where ϕ is the dimensionless electrostatic potential in units of kT/e in which k is Boltzmann's constant, T is the absolute temperature, e is the proton charge, ϵ is the dielectric constant, ρ^f is the fixed charge density, and I is the ionic strength of the bulk solution. The quantities ϕ , ϵ , and ρ are all functions of the position vector \mathbf{r} in the reference frame centered on a fixed macromolecule. For any system modeled with the NLPB equation, it has been shown that ΔG_{el} is given by a volume integral over all space (8):

$$\Delta G_{el} = \int \{ \rho^f \phi^f / 2 + \rho^f \phi^m + \rho^m \phi^m / 2 - (\rho^m \phi + kTc^b [2 \cosh(\phi) - 2]) \} dv, \quad [2]$$

where the potential, ϕ , and charge density, ρ , have been split up into contributions from the fixed, f , and the mobile, m , charges and c^b is the bulk salt concentration.

The electrostatic free energy of a macromolecule, described by Eq. 2, can be partitioned into salt-independent and salt-dependent terms. The salt-independent contribution to ΔG_{el} is given by (9, 10)

$$\Delta G_{ns} = \int (\rho^f \phi^f / 2) dv, \quad [3]$$

and the salt-dependent contribution to ΔG_{el} is given by (6)

$$\Delta G_s = \int \{ \rho^f \phi^m + \rho^m \phi^m / 2 - (\rho^m \phi + kTc^b [2 \cosh(\phi) - 2]) \} dv. \quad [4]$$

The interaction of an intercalating ligand with DNA can be analyzed as a two-step process:



In the first step, the B-DNA adopts the conformation of DNA in the complex, DNA*. In the second step, the ligand (L) binds to the unwound DNA. In the analyses presented here, we will evaluate the electrostatic free energy, $\Delta \Delta G_{el}$, of intercalating a charged and neutral ligand to an unwound DNA double helix (Eq. 6). Because of uncertainties in the structure of the free oligonucleotide, we will not be concerned with the contribution of structural changes in the DNA to $\Delta \Delta G_{el}$ (Eq. 6). We will, however, discuss some of the other consequences of DNA unwinding on our results.

The electrostatic contribution to the binding free energy can be expressed as the difference in the free energy between the products and the reactants (6):

$$\begin{aligned} \Delta \Delta G_{el} &= \Delta \Delta G_{ns} + \Delta \Delta G_s \\ &= \Delta G_{el}^{L \cdot \text{DNA}} - \Delta G_{el}^L - \Delta G_{el}^{\text{DNA}}. \end{aligned} \quad [7]$$

A physically intuitive description of the salt-independent contributions to $\Delta \Delta G_{el}$ is given by the thermodynamic process shown in Fig. 1 (10). In the initial state of this process, the fully solvated and charged molecules are infinitely separated from each other. In the first step, each molecule is partially desolvated by a low dielectric cavity (ϵ_m) corresponding to the region that the other molecule will come to occupy in the complex. The electrostatic free energy of this step is equal to the free energy of desolvating each molecule upon binding, $\Delta \Delta G_{d,L} + \Delta \Delta G_{d,DNA}$. In the following step, the charged molecules are transferred into the low dielectric cavity to form the final charged complex. The free energy of this step is given by the intermolecular solvent-screened coulombic interaction, $\Delta \Delta G_{sc}$. The thermodynamic process used to calculate the salt-dependent contributions to $\Delta \Delta G_{el}$ has been described in detail in a recent publication (6). $\Delta \Delta G_s$ can simply be interpreted as the change in the free energy of solvation of each molecule by salt in an aqueous environment (6).

Calculation of the pK_a shift of a single titratable group. The thermodynamic cycle shown in Scheme I describes the method used to calculate the pK_a of a single titratable group bound to DNA, pK_a^b , relative to the intrinsic pK_a of the group free in solution, pK_a^f . The shift in the pK_a of the group upon binding, ΔpK_a , is then

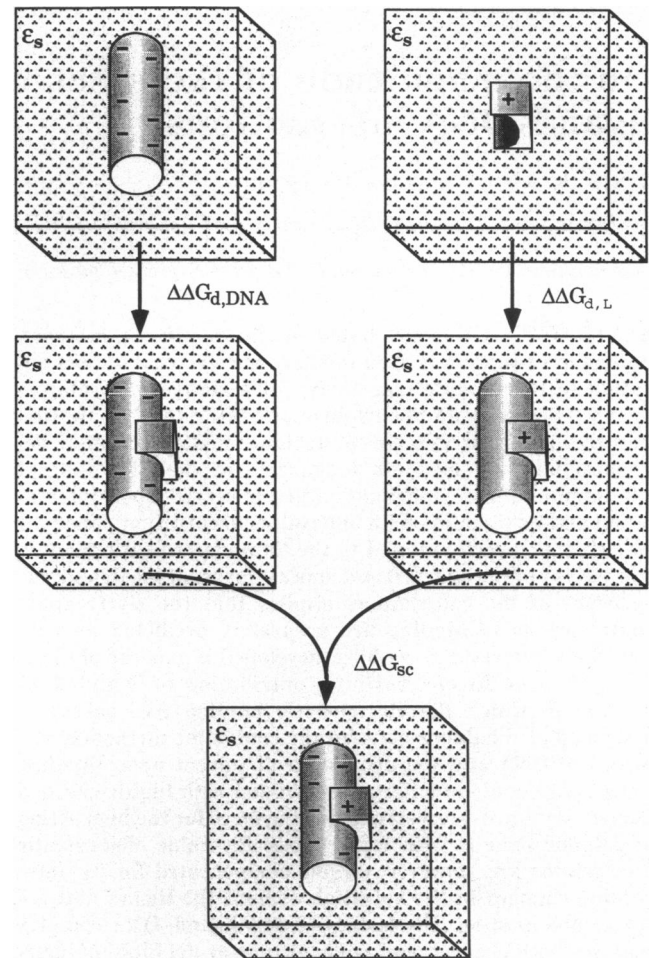
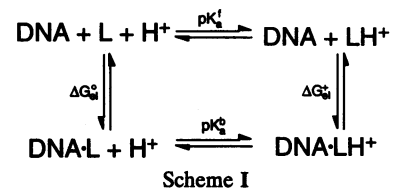


FIG. 1. The thermodynamic process for calculating the salt-independent contribution to the total electrostatic free energy of ligand-DNA binding, $\Delta \Delta G_{ns}$.



$$\Delta pK_a = pK_a^b - pK_a^f. \quad [8]$$

ΔpK_a is determined by the extra electrostatic free energy required to dissociate the proton from the ligand (L) in the environment of the nucleic acid relative to the reference state of the unbound ligand in solution. If the number of ligand-binding sites on the DNA is independent of pH, it is clear from Scheme I that the pK_a shift is determined by the relative electrostatic binding free energy of the DNA to the ligand in the protonated and unprotonated states:

$$\Delta pK_a = \frac{1}{2.3kT} (\Delta \Delta G_{el}^{\circ} - \Delta \Delta G_{el}^{+}), \quad [9]$$

where $\Delta \Delta G_{el}^{\circ}$ and $\Delta \Delta G_{el}^{+}$ are the electrostatic binding free energies, calculated according to Eq. 7, of the unprotonated and protonated ligand, respectively. Thus,

$$\Delta pK_a = \frac{1}{2.3kT} [(\Delta G_{L \cdot \text{DNA}}^{\circ} - \Delta G_{L \cdot \text{DNA}}^{+}) - (\Delta G_L^{\circ} - \Delta G_L^{+})], \quad [10]$$

where each ΔG in Eq. 10 is the electrostatic free energy of the molecule. Since ΔpK_a depends only on the electrostatic free energies of the protonated and unprotonated ligand in the bound and free states, we do not need to evaluate the free energy change of the DNA upon binding. The salt dependence of ΔpK_a depends only on the change in ΔG_s for the charged and neutral ligand upon binding. Therefore,

$$\frac{\partial \Delta pK_a}{\partial \ln[M^+]} = \frac{1}{2.3kT} \left(\frac{\partial \Delta \Delta G_s^+}{\partial \ln[M^+]} - \frac{\partial \Delta \Delta G_s^-}{\partial \ln[M^+]} \right), \quad [11]$$

where $[M^+]$ is the bulk univalent salt concentration.

Molecular Model. The details of the model used to describe the ligand and the DNA in the finite-difference NLPB method have been given in several publications (1, 3, 4, 11). The bound and free ligand in both the neutral and charged states are described by the x-ray crystallographic structure of the molecules described below. Each molecule is treated as a low dielectric cavity ($\epsilon_m = 4$) consisting of the volume enclosed by the solvent-accessible surface of the macromolecule obtained using a probe radius of 1.4 Å. A dielectric constant of 4 is used to account for both electronic polarization and small dipolar fluctuations that may accompany protonation in the macromolecule (1, 3, 12). The surrounding solvent was treated as a continuum of dielectric constant 80 with a 1:1 electrolyte behaving according to the NLPB equation. The atomic charges for the nucleic acid were derived directly from AMBER force-field parameters (13). The charges on the drug were derived from CVFF forcefield parameters (14) using a method of "bond increments" in the INSIGHT II software package (15). Charges were placed on the center of each atom. The mobile ions were excluded from the region <2.0 Å from the surface of each molecule (16).

An atomic resolution structure of DAPP bound to a 12-bp DNA was generated from the crystallographic coordinates of the ethidium-cytidylyl(3'-5')guanosine complex (17). The base pairs flanking the intercalation site were generated from the idealized local coordinates of Arnott and Hukins (18) using the INSIGHT II software package (15). The coordinates of idealized B-DNA were also generated from the local coordinates of Arnott and Hukins (18) using INSIGHT II. Before assigning partial charges to each atom, protons were added to each molecule, and the conformations were energy minimized using the molecular simulation program DISCOVER (15), with all heavy atoms fixed according to the modeled coordinates. The structures of the protonated and unprotonated forms of the complex were assumed to have similar conformations (2).

Numerical Calculations. Details of the finite difference procedure to calculate electrostatic potentials with the NLPB equation have been reported (4, 11, 19). To calculate the electrostatic potentials, the molecular system is first mapped onto a 129^3 lattice. Parameters are assigned to each lattice point according to the molecular model described above. The finite difference equations are solved by optimized successive overrelaxation to obtain the potential at all grid points (19). A simple two-step focusing procedure is used to improve the accuracy of the potentials (11). In the initial calculation, the largest dimension of the macromolecule fills 23% of the grid, and the potentials at the lattice points on the boundary of the grid are approximated analytically using the Debye-Hückel equation (16). The final potentials are calculated in two steps in which the grid is made 4 times finer, such that the largest dimension of the macromolecule fills 92% of the grid with the boundary conditions interpolated from the previous step. The final resolution for the ligand-DNA complexes was at least 2.0 grids per Å. At these resolutions, the final energies were found to vary by $<1\%$ with the position of the molecules on the grid. Each electrostatic free energy term (Eq. 7) is calculated from the electrostatic potentials at each lattice point using the

appropriate numerical integrals over the grid as described (4, 6, 10).

RESULTS

The pK_a Shift of the DAPP-DNA Complex. As shown in Fig. 2, the electrostatic interaction of DAPP with DNA shifts the pK_a of the ligand from a value of 5.8 in the free state (2) to more basic values in the bound state. For example, at 0.12 M $[M^+]$ ($\ln[M^+] = -2.12$), the experimentally observed pK_a of DAPP is shifted from 5.80 to 8.00 (Fig. 2). At this salt concentration, the calculated pK_a of the bound DAPP is shifted to 7.99 (Fig. 2; Table 1). The calculated pK_a of the ligand does not deviate from the experimental values by more than 0.10 unit at any salt concentration. The pK_a shift calculated with the NLPB equation also shows the same linear dependence on $\ln[M^+]$ (calculated slope = -0.39) as the experimental data (experimental slope = -0.34). Furthermore, the small curvature observed in both the experimental and theoretical lines occurs in the same direction (Fig. 2).

The Electrostatic Free Energy of Binding DAPP to DNA. Salt-independent contributions to $\Delta \Delta G_{el}$. The salt-independent contribution to $\Delta \Delta G_{el}$ for the intercalation of DAPP into the unbound DNA double helix (Eq. 6) is the sum of two opposing free energies, $\Delta \Delta G_{sc}$ and $\Delta \Delta G_d$. The solvent-screened intermolecular coulombic interaction, $\Delta \Delta G_{sc}$, between the DAPP and the DNA stabilizes both the protonated and unprotonated ligand in the complex (Table 1). In the unprotonated form of the ligand, this interaction arises from the small attraction of the partially charged dipolar groups on the DAPP to the DNA. These interactions include the electrostatic component of the hydrogen bonds between the DAPP amino groups and the DNA phosphate oxygens, so that $\Delta \Delta G_{sc}^+$ stabilizes the neutral DAPP-DNA complex by -1.2 kcal/mol. In the protonated form, the additional strong attraction between the positive charge on the phenanthridine ring and the negative charges on the DNA backbone substantially increases $\Delta \Delta G_{sc}$ to -9.4 kcal/mol. As a result, the contribution of the $\Delta \Delta G_{sc}$ to the pK_a shift of DAPP upon binding is 8.2 kcal/mol (Table 1).

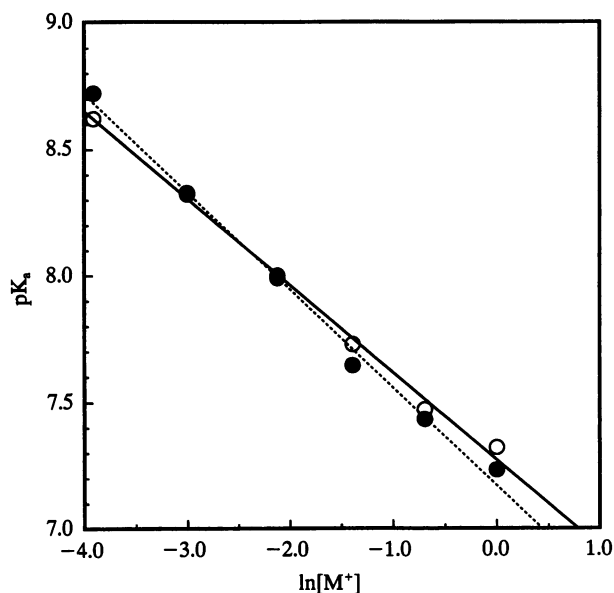


FIG. 2. The salt dependence of the pK_a of DAPP bound to DNA. ●, Absolute pK_a of the bound drug calculated with the NLPB equation (the experimental value of the pK_a of the free drug, 5.8, is added to the calculated values of the pK_a shift of DAPP upon binding). ○, Experimentally determined values of the absolute pK_a of DAPP in the ligand-DNA complex as reported by Jones and Wilson (2).

Table 1. Electrostatic free energy contributions to the DAPP–DNA interaction at 0.12 M [M^+]

Parameter	Free energy, kcal/mol			ΔpK_a^*
	L^+	L°	$L^\circ - L^+$	
$\Delta\Delta G_{sc}$	-9.4	-1.2	8.2	6.0
$\Delta\Delta G_{d,L}$	1.8	1.0	-0.8	-0.6
$\Delta\Delta G_{d,DNA}$	1.7	1.7	0.0	0.0
$\Delta\Delta G_{ns}$	-5.9	1.5	7.4	5.4
$\Delta\Delta G_s$	4.6	0.1	-4.5	-3.3
$\Delta\Delta G_{ei}$	-1.3	1.6	2.9	2.1

L^+ and L° , protonated and unprotonated states of DAPP, respectively; $L^\circ - L^+$, difference in the free energy between the unprotonated and protonated states of DAPP.

*The contribution of each term to the pK_a shift of DAPP upon binding calculated according to Eq. 10 at 25°C.

The favorable coulombic interaction driving the interaction between the DAPP and the nucleic acid is opposed by the desolvation of both the DNA and the ligand upon binding (Table 1). When DAPP binds to DNA, it buries both charged and polar groups on the DNA in the low dielectric molecular interface. This results in a small but significant desolvation free energy for the DNA, which opposes binding. The term $\Delta\Delta G_{d,DNA}$ is identical for both the charged and neutral ligand systems, since we have assumed that the structures of the protonated and unprotonated forms of the complex are similar. Therefore, $\Delta\Delta G_{d,DNA}$ does not contribute to the pK_a shift of DAPP upon binding.

The formation of a DAPP–DNA complex also buries both charged and polar groups on the ligand in the low dielectric interior of the DNA. The unfavorable desolvation free energy of the unprotonated DAPP upon binding, $\Delta\Delta G_{d,L}^\circ$, primarily reflects the removal of the polar DAPP amino groups from solvent. The term $\Delta\Delta G_{d,L}^+$ for the protonated DAPP is 0.8 kcal/mol larger than for the unprotonated molecule, since it includes the cost of desolvating an additional charge upon binding (Table 1). Thus, $\Delta\Delta G_{d,L}$ contributes -0.6 unit to the pK_a shift of DAPP upon intercalation (Table 1).

As a result of the desolvation of both the DNA and the ligand, the electrostatic free energy in the absence of salt, $\Delta\Delta G_{ns}$, actually opposes the formation of the unprotonated DAPP–DNA complex by 1.5 kcal/mol while $\Delta\Delta G_{ns}$ stabilizes the protonated DAPP–DNA complex by -5.9 kcal/mol (Table 1). The cumulative effect of the salt-independent contributions to the electrostatic free energy results in a pK_a shift of DAPP of 5.4 units upon binding (Table 1). As a result, in the absence of salt, the pK_a of DAPP is predicted to change from 5.8 in the free state to 11.2 in the bound state.

Salt-dependent contributions to $\Delta\Delta G_{ei}$. While salt has almost no effect on the binding of the unprotonated DAPP to DNA, it strongly opposes binding of the protonated DAPP, destabilizing the protonated DAPP–DNA complex by 4.6 kcal/mol at 0.12 M bulk salt concentration (Table 1). Salt effects result from a redistribution of cations and anions around each molecule upon binding (6). This ionic redistribution can have two causes. First, the presence of the ligand near the DNA can sterically exclude cations from high potential regions near the DNA. The small energetic consequences of physically moving these favorably interacting cations are seen in the binding of the neutral DAPP with DNA. Second, the binding of a positively charged ligand to the DNA electrostatically repels the cationic ion atmosphere around the DNA. The resulting dispersion of the ion atmosphere is ultimately responsible for the large salt-dependent contribution to $\Delta\Delta G_{ei}$ for the interaction of the protonated DAPP with DNA (6). At 0.12 M [M^+], $\Delta\Delta G_s$ opposes the protonation of the bound relative to the free ligand by 4.5 kcal/mol, resulting in a pK_a shift of DAPP of -3.3 units upon binding (Table 1). The magnitude of this effect depends on bulk salt concentration (Fig. 2). As bulk salt

concentration increases, the concentration of counterions near the DNA also increases. As a result, the unfavorable interaction between the protonated ligand and the ion atmosphere increases as well.

The total electrostatic binding free energy, $\Delta\Delta G_{ei}$. The relative stability of the DAPP–DNA complex depends on the charge state of the ligand (Fig. 3). The total electrostatic binding free energy, $\Delta\Delta G_{ei}$, for the intercalation of the neutral DAPP into the unwound DNA double helix is unfavorable at physiological ionic strengths (Fig. 3). This is because the desolvation of both the ligand and the DNA is not compensated for by the small favorable charge–dipole interactions between the unprotonated drug and the DNA upon binding (Table 1). In contrast, $\Delta\Delta G_{ei}$ for the intercalation of the charged DAPP is favorable at physiological ionic strengths (Fig. 3). The addition of a proton into the high negative potential of the DNA minor groove results in a substantially more favorable $\Delta\Delta G_{sc}$ with only a minor unfavorable change in the solvation free energy relative to the neutral drug (Table 1). Furthermore, while $\Delta\Delta G_s$ opposes the binding of the protonated DAPP more strongly than the unprotonated DAPP (Table 1), this effect does not destabilize the charged DAPP–DNA complex sufficiently to overcome the large value of $\Delta\Delta G_{sc}$ at physiological ionic strengths.

The binding of the charged drug to DNA, however, does grow progressively weaker with increasing bulk salt concentration, while the neutral drug–DNA interaction remains essentially salt independent (Fig. 3). The calculated value of the salt dependence, $\partial(\Delta\Delta G_{ei})/\partial\ln[M^+]$, for the intercalation of the protonated DAPP into the unwound DNA (Eq. 9) is 0.8. The value of $\partial(\Delta\Delta G_{ei})/\partial\ln[M^+]$ calculated here for the unwinding of the DNA (Eq. 8) is 0.4, so that the overall salt dependence of the binding of the protonated DAPP to DNA is found to be 1.2. This value agrees exactly with the experimentally observed salt dependence for the intercalation of the univalent ethidium molecule into DNA (20). We also predict that the overall salt dependence of the binding of the unprotonated DAPP to DNA is 0.4. This value is consistent with the experimentally observed salt dependence of 0.18 to 0.36 for the binding of electroneutral intercalators to DNA (21, 22).

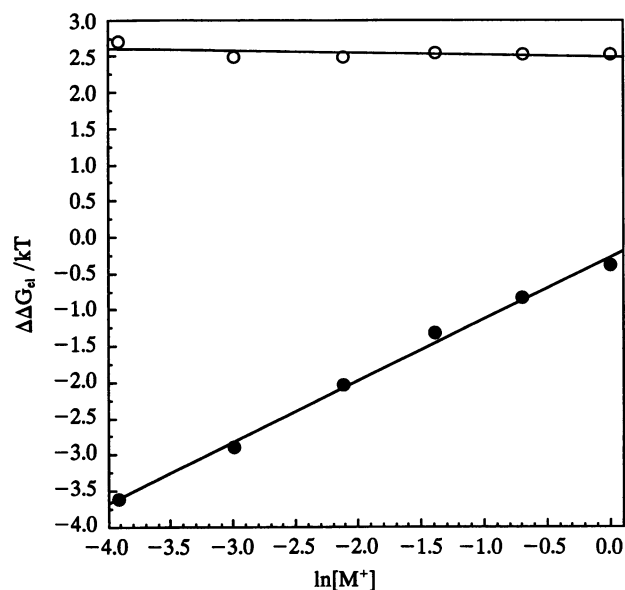


FIG. 3. The salt dependence of the total electrostatic free energy of binding ($\Delta\Delta G_{ei}$ expressed in units of kT) for the DAPP–DNA complex calculated with the NLPB equation. ●, Protonated ligand; ○, the unprotonated ligand.

DISCUSSION

The excellent agreement between our calculated values and the experimental values for the pK_a shift of DAPP bound to DNA shows that the NLPB model accurately describes both the magnitude and the salt dependence of electrostatic interactions between the macromolecules in an aqueous environment. As we have recently discussed, the physical description of electrostatic effects on ligand–DNA binding given by the NLPB model is very different from the traditional picture of “ion release” described by prior models (6). Both models correctly predict that binding decreases with increasing bulk salt concentration, c^b . However, in the NLPB model, charged ligand–DNA interactions are strongly opposed by the redistribution of salt, and the magnitude of this opposing force increases with c^b . In contrast, in ion-release models, binding is driven by the entropy of ion release, and the magnitude of this driving force decreases with c^b . We will discuss here the balance of electrostatic forces responsible for the binding of DAPP to DNA at physiological salt concentrations.

The coulombic attraction of DNA to cationic ligands drives binding. Local dipolar interactions, such as the hydrogen bonds between the DAPP amino groups and the DNA phosphate oxygens, can stabilize a ligand–DNA complex, as observed in the weak electrostatic attraction of the unprotonated DAPP with DNA (Table 1). However, the long-range coulombic forces associated with highly charged nucleic acids provide a much stronger driving force for the interaction of DNA with cationic ligands. For example, the solvent-screened coulombic interaction is found to drive the binding of the protonated DAPP to DNA by -9.4 kcal/mol (Table 1).

DNA-binding ligands exploit these long-range coulombic interactions with DNA. The positioning of the titrating proton on DAPP in the high negative potential grooves of the DNA optimizes its favorable intermolecular coulombic interactions without desolvating the charge in the binding interface. Proteins can use similar means to enhance DNA binding. In the *Escherichia coli* methionine repressor–operator system, a positively charged corepressor, *S*-adenosylmethionine, binds to a site distant from the DNA-binding interface and increases the affinity of the protein for its DNA by almost 1000-fold (23). These interactions have been found to be governed by the strong electrostatic attraction between *S*-adenosylmethionine and the DNA (24).

Coulombic interactions are, however, largely offset by changes in solvation of both the ligand and the DNA upon binding. The formation of a ligand–DNA complex removes both charged and polar groups at the binding interface from solvent while it displaces salt from around the nucleic acid. For the binding of the protonated DAPP to DNA, the desolvation of the molecules and the displacement of the ion atmosphere combine to oppose complexation by 8.0 kcal/mol, so that the total electrostatic binding free energy is a modest -1.3 kcal/mol at 0.12 M $[M^+]$. However, sterically bulky ligands can substantially increase the desolvation penalty of binding by burying both dipolar groups as well as phosphate charges on the DNA. Similarly, charges on the ligand can themselves become desolvated upon binding if they are located in the binding interface. Furthermore, additional positive charges on the ligand will electrostatically repel the ion atmosphere around DNA. In these cases, the desolvation of the ligand and the DNA upon binding can dominate the electrostatic interaction. Indeed, we have found that the binding of cationic ligands in the minor groove of DNA results in large penalties in both the solvation free energy (J. L. Hecht, V.K.M., and B.H., unpublished results) and the salt-dependent free energy (6) of binding. As a result, the electrostatic contribution to the binding free energy for these ligands actually opposes binding (J. L. Hecht, V.K.M., and B.H., unpublished results).

The relatively small electrostatic free energy of binding a positively charged ligand to DNA is not expected to be large enough to offset the entropic cost of losing six translational and rotational degrees of freedom upon complex formation (25). This unfavorable entropic free energy must be compensated by other interactions. Nonpolar interactions, involving both tight packing and the hydrophobic effect, have been shown to be an important driving force for the binding of several minor-groove-binding ligands (26, 27) and proteins (28–30) to DNA. Both tight packing and hydrophobic effects are related to the removal of nonpolar surface on complex formation (1, 28). For the intercalation of DAPP to the unwound DNA double helix, about 600 Å² of total surface area is buried in the drug–DNA interface upon complexation. This effect is, of course, modified by the exposure of surface area during the unwinding of the double helix before binding. Nevertheless, nonpolar interactions appear to provide a large driving force for the intercalation of DAPP into DNA, which can, in fact, offset the entropic cost of complex formation.

We thank Drs. Richard Friedman and An-Suei Yang for their many helpful insights and discussions regarding this work. This work was supported by National Institutes of Health Grant GM-41371.

- Honig, B., Sharp, K. & Yang, A. (1993) *J. Phys. Chem.* **97**, 1101–1109.
- Jones, R. L. & Wilson, W. D. (1981) *Biopolymers* **20**, 141–154.
- Sharp, K. A. & Honig, B. (1990) *Annu. Rev. Biophys. Biophys. Chem.* **19**, 301–332.
- Jayaram, B., Sharp, K. A. & Honig, B. (1989) *Biopolymers* **28**, 975–993.
- Misra, V. K., Hecht, J. L., Sharp, K. A., Friedman, R. A. & Honig, B. (1994) *J. Mol. Biol.* **238**, 264–280.
- Misra, V. K., Sharp, K. A., Friedman, R. A. & Honig, B. (1994) *J. Mol. Biol.* **238**, 245–263.
- Zacharias, M., Luty, B. A., Davis, M. E. & McCammon, J. A. (1992) *Biophys. J.* **3**, 1280–1285.
- Sharp, K. A. & Honig, B. (1990) *J. Phys. Chem.* **94**, 7684–7692.
- Gilson, M. K., Rashin, A., Fine, R. & Honig, B. (1985) *J. Mol. Biol.* **183**, 503–516.
- Gilson, M. K. & Honig, B. (1988) *Proteins Struct. Funct. Genet.* **4**, 7–18.
- Gilson, M. K., Sharp, K. A. & Honig, B. H. (1988) *J. Comput. Chem.* **9**, 327–335.
- Harvey, S. (1988) *Proteins Struct. Funct. Genet.* **5**, 78–92.
- Weiner, S. J., Kollman, P. A., Nguyen, D. T. & Case, D. A. (1986) *J. Comput. Chem.* **7**, 230–252.
- Hagler, A. T., Stern, P. S., Sharon, R., Becker, J. M. & Naider, F. (1979) *J. Am. Chem. Soc.* **101**, 6842–6852.
- Biosym (1992) *INSIGHT II* (Biosym Technologies, San Diego).
- Klapper, I., Hagstrom, R., Fine, R., Sharp, K. & Honig, B. (1986) *Proteins Struct. Funct. Genet.* **1**, 47–59.
- Jain, S. C. & Sobell, H. M. (1984) *J. Biomol. Struct. Dyn.* **1**, 1179–1195.
- Arnott, C. F. & Hukins, D. W. (1972) *Biochem. Biophys. Res. Commun.* **47**, 1504–1509.
- Nicholls, A. & Honig, B. (1991) *J. Comp. Chem.* **12**, 435–445.
- Wilson, W. D., Krishnamoorthy, C. R., Wang, Y.-H. & Smith, J. C. (1985) *Biopolymers* **24**, 1941–1961.
- Chaires, J. B., Priebe, W., Graves, D. E. & Burke, T. G. (1993) *J. Am. Chem. Soc.* **115**, 5360–5364.
- Friedman, R. A., Manning, G. S. & Shahin, M. A. (1990) in *The Polyelectrolyte Correction to Site-Exclusion Numbers in Drug-DNA Binding*, ed. Kallenbach, N. R. (Adenine, New York), pp. 37–64.
- Phillips, S. E. V., Manfield, I., Parsons, I., Davidson, B. E., Rafferty, J. B., Somers, W. S., Margarita, D., Cohen, G. N., Saint-Girons, I. & Stockley, P. G. (1989) *Nature (London)* **341**, 711–720.
- Phillips, K. & Phillips, S. E. V. (1994) *Structure* **2**, 309–316.
- Finkelstein, A. V. & Janin, J. (1989) *Protein Eng.* **3**, 1–3.
- Ding, W.-D. & Ellestad, G. A. (1991) *J. Am. Chem. Soc.* **113**, 6617–6620.
- Boger, D. L., Invergo, B. J., Coleman, R. S., Zarrinmayer, H., Kitos, P. A., Thompson, S. A., Leong, T. & McLaughlin, L. W. (1990) *Chem. Biol. Interact.* **73**, 29–52.
- Spolar, R. S. & Record, M. T. J. (1994) *Science* **263**, 777–784.
- Ha, J.-H., Spolar, R. S. & Record, M. T. (1989) *J. Mol. Biol.* **209**, 801–816.
- Lundback, T., Cairns, C., Gustafsson, J.-A., Carlstedt-Duke, J. & Hard, T. (1993) *Biochemistry* **32**, 5074–5082.